

Research Article

Raman Spectroscopic Characterization of Endodontic Biofilm Matrices

Tatiana Ramirez-Mora ¹, Claudia Dávila-Pérez,² Fernando Torres-Méndez,² and Grettel Valle-Bourrouet³

¹Restorative Department, Faculty of Dentistry, University of Costa Rica, San Pedro Montes de Oca 11801, Costa Rica

²Endodontics Postgraduate Program, Faculty of Dentistry, University of San Luis Potosí, San Luis Potosí 78290, Mexico

³Inorganic Chemistry Department, School of Chemistry, University of Costa Rica, San Pedro Montes de Oca 11801, Costa Rica

Correspondence should be addressed to Tatiana Ramirez-Mora; tatiana.ramirez@ucr.ac.cr

Received 2 September 2018; Revised 14 November 2018; Accepted 12 December 2018; Published 10 January 2019

Academic Editor: Austin Nevin

Copyright © 2019 Tatiana Ramirez-Mora et al. This is an open access article distributed under the Creative Commons Attribution License, which permits unrestricted use, distribution, and reproduction in any medium, provided the original work is properly cited.

Endodontic persistent infections are often mediated by bacterial biofilms. This mode of bacterial growth is characterized by the presence of a matrix mainly composed of extracellular polymeric substances (EPSs) that protect the encased microorganisms. To establish better control and disinfection protocols, elucidation of the main components of biofilm matrices present in endodontic infections is required. The aim of the present study was to characterize the principal components of *E. faecalis*, *A. naeslundii*, and dual-species biofilm matrices by means of Raman spectroscopy and confocal scanning laser microscopy (CSLM) techniques. The total biomass of biofilms was quantified via crystal violet assays, and the monospecies biofilms showed higher biomass than the dual-species biofilms. Raman spectroscopy and confocal laser scanning microscopy were used to identify the biochemical composition and structure of the biofilm matrices. Spectra originating from the biofilms of two endodontic pathogens show the presence of carbohydrates, proteins, fatty acids, and nucleic acids in all samples; however, variation in the levels of expression of these biomolecules allows spectroscopic differentiation of the biofilms using principal component analysis. This study is the first attempt to identify the composition of monospecies and dual-species biofilms of endodontic origin. Our data provides an important approach to the understanding of molecular dynamics of endodontic infections.

1. Introduction

Microbiota diversity of persistent endodontic infections is very limited, and Gram-positive facultative bacteria are commonly isolated [1, 2]. *Enterococcus faecalis* and *Actinomyces* spp. represent two of the species most frequently isolated from specimens of this clinical condition [2, 3]. Both have the ability to form biofilms, which confers on them the ability to persist despite harsh environmental conditions such as root canal chemomechanical disinfection, intracanal medication, and even antibiotic therapy [4].

The occurrence of biofilms in infected root canals and elsewhere has been widely reported; morphological investigations of teeth with primary or persistent apical periodontitis have revealed the presence of biofilms not only

in the main root canal but also within anatomical variations including lateral canals, isthmuses, and apical ramifications [5, 6]. Extraradicular biofilms attached to the external surface of the root in case of endodontic treatment failure have also been described [7, 8].

Bacterial biofilms are surface-associated communities that produce a variety of macromolecules. These so-called extracellular polymeric substances (EPSs), such as polysaccharides, proteins, fatty acids, and extracellular DNA (eDNA) [9], provide the structural and functional integrity of the biofilm matrix and are also involved in communication processes, genetic transfer, nutrition, and the interaction of the bacteria with their environment [10, 11]. The production and type of EPS is influenced by different factors such as bacterial species, environmental conditions, nutrient

availability, adhesion surface, etc. [12]. These factors are the origin of high diversity and multiple types of biofilms, and this heterogeneity is the main cause of the pathogenesis of many chronic and life-threatening infections [13].

Since biofilm matrices vary greatly, many methods and techniques may be used to study their ultrastructure and chemical composition. Microscopy techniques such as scanning electron microscopy (SEM), atomic force microscopy (AFM), transmission electron microscopy (TEM), and confocal laser scanning microscopy (CLSM) are among the methods employed to determine biofilm matrix structure [14]. Recently, CSLM has become a very popular and useful tool for in situ assessment of biofilm structure and detection of matrix components using different staining protocols [15]. However, chemical information provided by CSLM can be limited because of missing interactions between stains and compounds, and it is also an expensive and highly time-consuming technique.

Raman microscopy, a molecular vibration-based spectroscopic technique, is a powerful analytical tool for the study of biological materials. It allows rapid, in situ, non-invasive acquisition of chemical and structural information through the generation of fingerprint spectra. Ivleva et al., Popp and coworkers, and other research groups have employed Raman spectroscopy for chemical analysis of biofilms, differentiation of planktonic and biofilm cells, discrimination of diverse species of bacteria in biofilms, and monitoring metabolic characteristics under different physiologic states [16–19].

In the field of endodontics, a previous study used Raman spectroscopy to analyse the chemical compositions of *E. faecalis* biofilms in different physiological states in which the matrix components differed according to the growth phase [20]. This study provided important information about monospecies biofilm composition; nevertheless, root canal infections are clearly mediated by monospecies, dual-species, or multispecies biofilms [8, 12, 21], and therefore it is necessary to investigate monospecies and dual species of different relevant root canal bacteria, especially those involved in persistent periapical pathosis. Data resulting from such studies could represent a valuable contribution to the establishment of a new understanding and the determination of strategies to prevent and eradicate biofilms from the root canal system. In this context, the present study was designed to combine Raman spectroscopy and confocal laser scanning microscopy techniques to obtain biochemical composition from monospecies and dual-species endodontic biofilms.

2. Materials and Methods

2.1. Bacterial Strains and Media. *E. faecalis* and *A. naeslundii* strains, from persistent endodontic infections, were used. Samples were incubated inside an anaerobic chamber (85% N₂, 10% H₂, 5% CO₂; Coy Laboratory Products, Grass Lake, MI, USA). Identification was performed using specific agar media and API biochemical tests. Confirmation of the identity and antibiotic resistance was performed with the VITEK 2 automated system (BioMérieux®, Cambridge, MA, USA).

2.2. Biofilm Assays. Biofilm assays were conducted based on a previously reported method [22]. After confirmation of the strain purity by Gram staining and colony morphology, a single colony of each bacterial strain was inoculated in 10 mL of brain heart infusion (BHI) and cultured overnight at 37°C. For the monospecies suspension, the cell density was 10⁹ cells/mL (OD = 1, as measured using a Pharmacia LKB Ultrospec III spectrophotometer). A mixed microbial suspension was prepared in a sterile falcon tube from equal volumes of *E. faecalis* and *A. naeslundii* suspensions (OD = 1) to grow the dual-species biofilms. For the biofilm formation, a 0.2 mL inoculum was transferred to a 24-well polystyrene tissue culture plate (Sarstedt Inc., Newton, NC, USA) containing 1.8 mL of BHI, and the biofilms were then grown under static and anaerobic conditions (85% N₂, 10% H₂, 5% CO₂; Coy Laboratory Products Inc., Grass Lake, MI, USA) for 14 days. The growth media was replaced every second day to remove dead cells and provide nutrition.

For biofilm EPS visualization of each sample via CSLM, glass coverslips (Thermo Fisher Scientific, Waltham, MA, USA) were placed in a 24-well culture plate and grown in triplicate.

2.3. Biofilm Quantification Assay. Formation of monospecies and dual-species biofilms was quantified using the crystal violet (CV) method [23] with slight modifications. *E. faecalis*, and *A. naeslundii* that had been grown overnight were diluted 1:100 in the BHI medium, and for each cell suspension, 200 µL was transferred to a sterile flat-bottomed 96-well polystyrene plate. For the dual-species biofilm, 100 µL of each cell suspension was added per well. After stationary anaerobic incubation at 37°C for 14 days, the broth was carefully aspirated, and then the wells were washed three times with 200 µL PBS and air-dried for 30 min at room temperature. The biofilms were then stained with 200 µL of 1% crystal violet, under constant agitation for 15 min at room temperature, and washed again with PBS (three times), and the bound crystal violet solubilized in 200 µL of 95% ethanol for 10 min. Thereafter, the optical density (OD) was measured at 570 nm (OD₅₇₀) using a microtiter plate reader (Bio-Tek Synergy HT). Biofilm mass was expressed as OD 570 nm values. The assay was repeated three times.

2.4. EPS Identification via CLSM. CLSM was used for the identification of EPSs within the biofilm matrix. After incubation for 14 days, the glass coverslips were washed twice with phosphate-buffered saline (PBS). Next, the biofilms were incubated in a staining mixture for 15 min in dark. Calcofluor and propidium iodide (Sigma-Aldrich Co. St. Louis, MO, USA) were used as fluorescent stains for polysaccharide and eDNA, respectively. Following this, the biofilms were washed in PBS to remove excess stain. Before the biofilms were completely dry, a mounting medium was applied. Confocal analysis was performed using an Olympus U-TB190 (100×) microscope objective under oil immersion. Confocal images of 1024 × 1024 pixels were acquired with

the FV10-AV version 03.01 software (Olympus, Japan) and assembled using Adobe Photoshop CS3 (Adobe Systems).

2.5. Biofilm EPS Extraction. Biofilm EPSs were extracted as previously described [24] with slight modifications. Biofilms were recovered from the tissue flask by scraping (Falcon cell scraper, Corning Science Mexico, Reynosa, Tamps., Mexico), suspended in PBS (10 mL), transferred to polypropylene conical tubes (BD), and vortexed for 1 min. Next, the biofilm samples were sonicated in an ultrasonic bath (Branson 5800, Emerson, St. Louis, MO, USA) for 45 min, followed by vortexing for 2 min, and then centrifuged (3500 rpm; 15 min) (Sorvall Legend X1R, Thermo Fisher Scientific, Waltham, MA, USA). The supernatant fraction was recovered and filtered through 0.2 μm Acrodisc[®] syringe filters with Supor[®] Membrane (Pall Life Sciences, Deland, FL, USA).

Biofilm samples were transferred to quartz slides with a 10 μL inoculating loop. The smears were dried for 20 min with silica.

2.6. Spectroscopy Instrumentation and Measurement. All Raman spectra were recorded using a Raman microspectrometer (ProRaman-L, Enwave Optronics Inc., Irvine, CA, USA). A 50 \times microscope objective (Leica Microsystems Inc., Buffalo Grove, IL, USA) was used, and the samples were excited using 45–50 mW of a 785 nm diode laser. The Raman signal was collected in the spectral interval 600–1800 cm^{-1} ; the integration time was 40 s, and spectral resolution was approximately 2 cm^{-1} . To record biofilm Raman spectra, on each smear of the quartz slides, a central focus point was selected, and around this centre, spectra were collected at ten points for each sample.

2.7. Spectral Preprocessing and Analysis. Spectra were processed via customized Raman processing software [25] and Origin 8.0 (OriginLab Corp., Northampton, MA, USA). Each Raman spectrum was first processed by using a median filter to remove cosmic rays and noise. Spectral intensities were normalized to the range of 0–1 arbitrary units, and an automated polynomial baseline correction method was applied. The Raman spectra were then analysed via multivariate techniques, namely, principal component analysis (PCA) and discriminant function analysis (DFA).

3. Results and Discussion

Biofilm quantification assay of the monoculture biofilms was compared to the dual-species biofilms. Both species *E. faecalis* and *A. naeslundii* had the ability to form biofilms under the experimental conditions. The criteria used to categorize biofilm formation capacity were based on the approach of previous researchers [26, 27]. According to them, both species can be categorized as “biofilm formers.” Mean OD 570 nm values of monoculture biofilms were higher compared to the values of dual-species biofilms (Figure 1). It has been reported that, for bacteria that grow

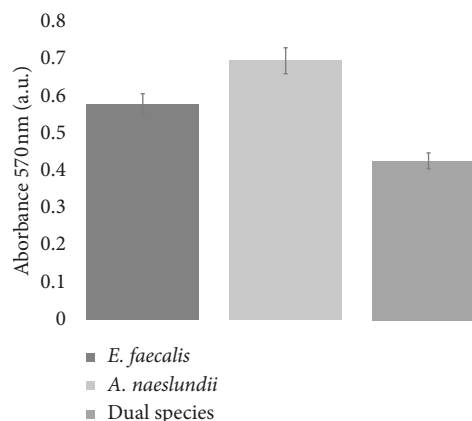


FIGURE 1: Crystal violet quantification of monoculture and dual-species biofilms of *E. faecalis* and *A. naeslundii* bacteria. Data represent mean \pm SD of triplicate readings.

similarly well in the monoculture model, slight decreases can be expected for both components when grown in dual-species biofilms [28]. However, a recent study reported that when Gram-positive bacteria were cocultured with Gram negative, dual-species biofilms showed higher values compared to monoculture biofilms of Gram-negative bacteria [29]. It could be explained based on the fact that different bacterial cell-cell interrelation may exist when growing in cocultured biofilms, including competition, synergism, and nutrients availability [28, 30].

Our findings suggest the presence of the principal biomolecules that have been previously described as components of EPS biofilm matrices [11]. Furthermore, based on the intensity of the Raman bands, we were able to describe the EPS composition as dominated by a major protein fraction, with saturated fatty acids and polysaccharides occurring in a relatively smaller proportion, and a minor nucleic acid component. This composition reflects the characteristic of a mature biofilm as previously reported by other authors [20, 31, 32]. In another Raman spectroscopic study, Huang et al. found that the amide I region was more intense in the stationary phase than in the exponential phase [33]. Liu et al. reported that changes in nucleic acid and protein bands reflected the physiologic state of *E. faecalis* biofilms [20].

In the past, polysaccharides were considered to be almost the only structural component of the extracellular matrix, until further research elucidated another important structural biomolecule, eDNA [33]. Thus, in the present study, both components were characterized by means of CLSM. Calcofluor was used to perform polysaccharide staining, and propidium iodide for eDNA staining. CLSM images revealed the presence of polysaccharide clumps and eDNA fibres as components of the biofilm matrix. Mushroom-shaped structures and water channels, characteristics of mature biofilms, were also identified [34]. It has been proposed that eDNA can play distinct roles: first, as an adhesin in the early stages of biofilm formation, and second, as a structural component of the mature biofilm [35–37]. Figure 2 shows CSLM images of the developed biofilms at a mature stage, in

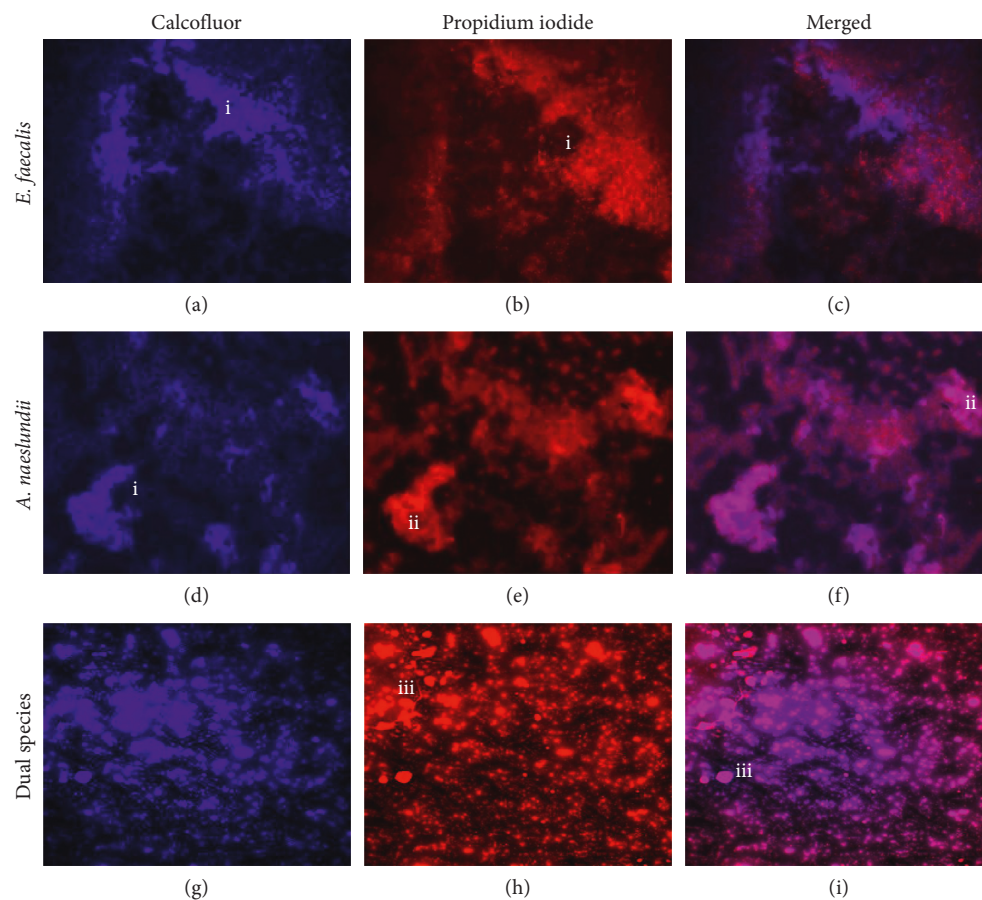


FIGURE 2: CSLM figures of biofilm matrices. Polysaccharides clumps (a, d, e) and eDNA aggregates (b, c, h). Structural features such as water channels (i), mushroom-like forms (ii), and eDNA fibres (iii) were identified.

which the presence of polysaccharides and eDNA as EPS matrix components was observed.

In spite of the similarity of the spectra of the different biofilms and the fact that both are Gram-positive bacteria, a PCA-DFA canonical plot of the Raman spectral profile data for the three biofilms suggests that *E. faecalis*, *A. naeslundii*, and the dual-species biofilm have extracellular matrices with different biochemical compositions; the cross-validation value was 95.1%. The main spectral differences are noticed in the spectral bands around $1270\text{--}1335\text{ cm}^{-1}$ and $1000\text{--}1125\text{ cm}^{-1}/800\text{--}980\text{ cm}^{-1}$, which are assigned to protein and polysaccharides biomolecules, respectively (Figures 3(a) and 3(b)).

In a previous research, we found that biochemical composition among these biofilms species varies significantly from monospecies to dual species [38]. A major fraction of polysaccharides, proteins, and fatty acids was identified in the monospecies biofilms compared to those in the dual-species biofilms [38]. These results indicate that the two species influence each other at the biochemical level, and further data support the synergistic action between these two endodontic pathogens [39].

Figure 3(b) shows Raman spectra of the EPSs extracted from the three samples. Raman bands were assigned and interpreted based on previous research [15, 17, 40, 41]. Functional groups from the main biomolecules were

identified (Figure 4). The bands in the region of $790\text{--}950\text{ cm}^{-1}$ can be attributed to side-group deformations (COH, CCH, and OCH) in biofilm-specific polysaccharides [15]. Raman spectra of the EPS fractions of the three biofilm samples showed variation in this region; the *E. faecalis* spectra were particularly different. Biofilm polysaccharides can vary greatly in their composition, which is mostly defined by factors such as genetic profile and environmental growth conditions. In Gram-positive cells, the presence and chemical structure of many rhamnase-containing cell-wall polysaccharides (RhaCWP) has been known for decades. The bands observed at $880\text{--}980$, 1055 , and 1075 cm^{-1} could be tentatively assigned to a combination of vibrational modes of rhamnose, galactose, and glucose [40]. Previous studies have reported the presence of these saccharides as part of *E. faecalis* as well as *Actinomyces* spp. [42–44].

The bands in the $1075\text{--}1125\text{ cm}^{-1}$ region can be assigned to the C–C and C–N stretching vibration contributions [15, 18, 19]. Amide I (the $1640\text{--}1680\text{ cm}^{-1}$ stretching vibration of C=O) and amide III (1250 cm^{-1} , associated with C–N stretching and N–H bending) bands were detected in the three biofilm spectra; however, the intensities of the bands varied significantly among them. The *A. naeslundii* spectra show an intense band around 1300 cm^{-1} (amide III), but this has also been assigned to the amino acid side-chain mode of tryptophan. It

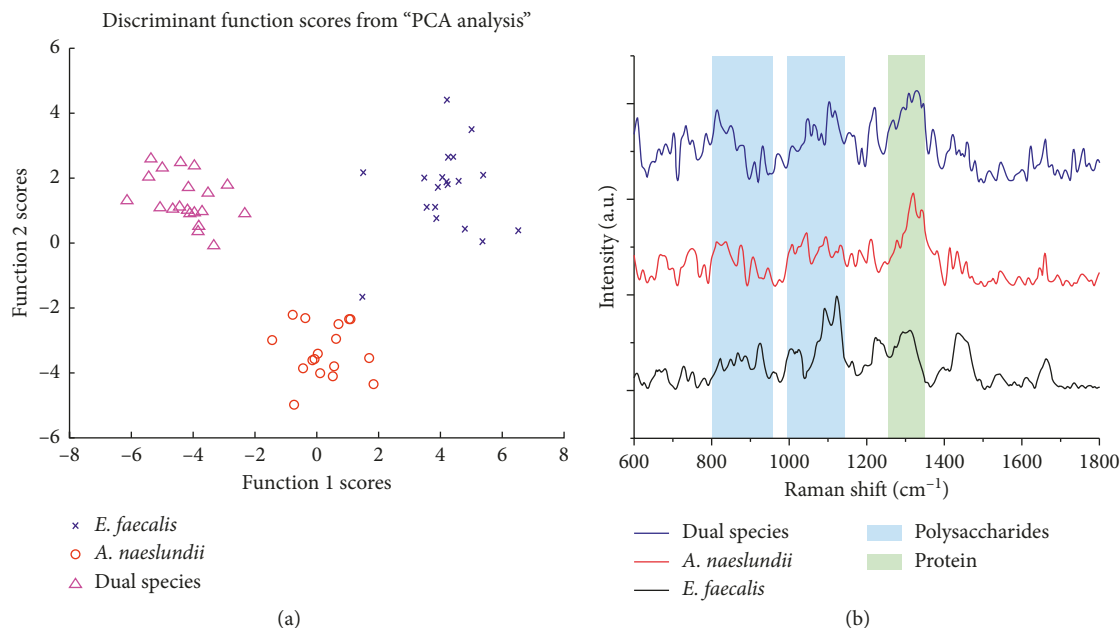


FIGURE 3: Raman spectroscopic analyses of *E. faecalis*, *A. naeslundii*, and dual biofilms (a). A PCA-DFA plot of all the Raman spectra from the biofilm developed from *E. faecalis* (asterisk), *A. naeslundii* (circle), and dual species (triangle). The value of cross-validation was 95.1%. Principal spectral differences can be seen in three main ranges (b).

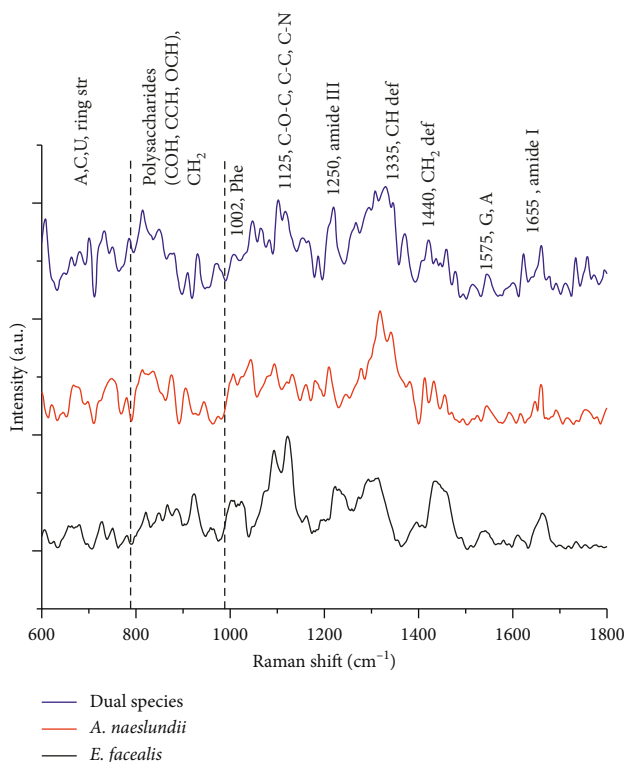


FIGURE 4: Raman spectra of three biofilm matrix samples. Functional groups from biomolecules were identified.

has been demonstrated that proteins contribute to initial adhesion and stability of the biofilm matrix [44]. Thus, there is a possibility that the bands related to proteins could represent lectins and amyloid-like proteins, a group of

proteins that have been identified in many species implicated in biofilm formation [44–46]. These molecules can recognize carbohydrates in biofilm matrices and promote cell-to-cell communication. Raman spectra of lyophilized lectins show some bands at different positions, for instance, those around 1667 cm^{-1} and 1236 cm^{-1} , in the amide I and amide III bands, respectively [47]. Amyloids are involved in the building and stability of biofilm matrices. The term “amyloid” describes β -sheet-rich protein aggregates, which exhibit Raman bands mainly in the amide I ($1665\text{--}1680\text{ cm}^{-1}$) and amide III ($1246\text{--}1270\text{ cm}^{-1}$) regions [47, 48]. All of these bands were observed in the EPS samples analysed in the present study.

Since 2002, the functional role of eDNA in biofilm formation and structural integrity has been established [36], and the presence of bands attributable to the DNA backbone has been reported in previous research on biofilms [20]. Our findings reveal the presence of small bands around 728 , 780 , and 785 cm^{-1} , assigned to adenine, cytosine, and uracil, respectively [15]. Moreover, a band at 1575 cm^{-1} characteristic of guanine and adenine ring stretching [17] was identified in all our EPS samples.

The most distinctive features of the Raman spectra of lipids are related to the presence of the hydrocarbon chains, and for all lipids, these can be observed in the following regions: $1500\text{--}1400$, $1300\text{--}1250$, and $1200\text{--}1050\text{ cm}^{-1}$, which is in the fingerprint region [49]. In the present study, bands around 1445 and 1500 cm^{-1} assigned to scissoring vibrations of the CH_2 group were identified. Furthermore, the Raman band at 1300 cm^{-1} , attributed to the twisting vibration of the CH_3 group, is particularly intense in the spectrum of palmitic acid [49]. The presence of fatty acids has been reported in

bacterial biofilms, especially saturated fatty acids [15, 18, 26]. Moreover, in a fatty acid profile of the initial oral biofilm, palmitic (16:0), stearic (18:0), oleic (18:1n9c), and erucic (22:1n9c) acids were detected [50]. These fatty acids have intense bands in the 1400–1500 cm^{-1} region due to the CH_2/CH_3 deformation modes, similar to bands found in our study [15, 51].

4. Conclusions

As a preliminary study, our results showed variations in wave shape confirming the difference in the chemical composition of analysed biofilms, although more data are obviously required on the biofilm molecular composition when grown on biological surfaces including dentin or hydroxyapatite. It is of interest to examine metabolic activities of bacteria during the maturation of the biofilm process, especially in mixed populations where interspecies interactions show different chemical behavior [29, 38].

Raman spectroscopic and CSLM technique allowed the biochemical and structural characterization of monospecies and dual-species biofilm matrices. Our results provide valuable information about EPS matrix components of relevant biofilm-forming endodontic bacteria, elucidating the variability and complexity that prevail in microbial communities. These data represent the first approach, and further research will be necessary to confirm and clearly identify the EPS components that we tentatively identified in this study.

Data Availability

The data used to support the findings of this study are available from the corresponding author upon request.

Conflicts of Interest

The authors declare that there are no conflicts of interest regarding the publication of this paper.

Acknowledgments

The study was approved by the Institutional Ethics Committee of the Faculty of Dentistry at San Luis Potosi University, San Luis Potosi, México (Approval Code CEI-FE-011-014).

References

- [1] C. Zhang, J. Du, and Z. Peng, "Correlation between *Enterococcus faecalis* and persistent intraradicular infection compared with primary intraradicular infection: a systematic review," *Journal of Endodontics*, vol. 41, no. 8, pp. 1207–1213, 2015.
- [2] L. C. de Paz, "Redefining the persistent infection in root canals: possible role of biofilm communities," *Journal of Endodontics*, vol. 33, no. 6, pp. 652–662, 2007.
- [3] F. G. C. Signoretti, M. S. Endo, B. P. F. A. Gomes, F. Montagner, F. B. Tosello, and R. C. Jacinto, "Persistent extraradicular infection in root-filled asymptomatic human tooth: scanning electron microscopic analysis and microbial investigation after apical microsurgery," *Journal of Endodontics*, vol. 37, no. 12, pp. 1696–1700, 2011.
- [4] L. Chavez de Paz, "Gram-positive organisms in endodontic infections," *Endodontic Topics*, vol. 9, no. 1, pp. 79–96, 2004.
- [5] P. N. R. Nair, S. Henry, V. Cano, and J. Vera, "Microbial status of apical root canal system of human mandibular first molars with primary apical periodontitis after "one-visit" endodontic treatment," *Oral Surgery, Oral Medicine, Oral Pathology, Oral Radiology, and Endodontology*, vol. 99, no. 2, pp. 231–252, 2005.
- [6] D. Ricucci and J. F. Siqueira, "Apical actinomycosis as a continuum of intraradicular and extraradicular infection: case report and critical review on its involvement with treatment failure," *Journal of Endodontics*, vol. 34, no. 9, pp. 1124–1129, 2008.
- [7] L. Tronstad and P. T. Sunde, "The evolving new understanding of endodontic infections," *Endodontic Topics*, vol. 6, no. 1, pp. 57–77, 2003.
- [8] G. Svensater and G. Bergholtz, "Biofilms in endodontic infections," *Endodontic Topics*, vol. 9, no. 1, pp. 27–36, 2004.
- [9] P. Stoodley, K. Sauer, D. G. Davies, and J. W. Costerton, "Biofilms as complex differentiated communities," *Annual Review of Microbiology*, vol. 56, no. 1, pp. 187–209, 2002.
- [10] H.-C. Flemming, T. R. Neu, and D. J. Wozniak, "The EPS matrix: the "house of biofilm cells"," *Journal of Bacteriology*, vol. 189, no. 22, pp. 7945–7947, 2007.
- [11] H.-C. Flemming and J. Wingender, "The biofilm matrix," *Nature Reviews Microbiology*, vol. 8, no. 9, pp. 623–633, 2010.
- [12] S. George, A. Kishen, and P. Song, "The role of environmental changes on monospecies biofilm formation on root canal wall by *Enterococcus faecalis*," *Journal of Endodontics*, vol. 31, no. 12, pp. 867–872, 2005.
- [13] R. M. Donlan, "Biofilms: microbial life on surfaces," *Emerging Infectious Diseases*, vol. 8, no. 9, pp. 881–890, 2002.
- [14] E. Denkhaus, S. Meisen, U. Telgheder, and J. Wingender, "Chemical and physical methods for characterisation of biofilms," *Microchimica Acta*, vol. 158, no. 1-2, pp. 1–27, 2006.
- [15] M. Wagner, N. P. Ivleva, C. Haisch, R. Niessner, and H. Horn, "Combined use of confocal laser scanning microscopy (CLSM) and Raman microscopy (RM): investigations on EPS-matrix," *Water Research*, vol. 43, no. 1, pp. 63–76, 2009.
- [16] N. P. Ivleva, M. Wagner, H. Horn, R. Niessner, and C. Haisch, "Towards a nondestructive chemical characterization of biofilm matrix by Raman microscopy," *Analytical and Bioanalytical Chemistry*, vol. 393, no. 1, pp. 197–206, 2008.
- [17] M. Harz, P. Rösch, and J. Popp, "Vibrational spectroscopy—a powerful tool for the rapid identification of microbial cells at the single-cell level," *Cytometry Part A*, vol. 75A, no. 2, pp. 104–113, 2009.
- [18] D. Kusić, B. Kampe, A. Ramoji, U. Neugebauer, P. Rösch, and J. Popp, "Raman spectroscopic differentiation of planktonic bacteria and biofilms," *Analytical and Bioanalytical Chemistry*, vol. 407, no. 22, pp. 6803–6813, 2015.
- [19] C. Sandt, T. Smith-Palmer, J. Pink, L. Brennan, and D. Pink, "Confocal Raman microspectroscopy as a tool for studying the chemical heterogeneities of biofilms in situ," *Journal of Applied Microbiology*, vol. 103, no. 5, pp. 1808–1820, 2007.
- [20] H. Liu, Q. Xu, L. Huo, X. Wei, and J. Ling, "Chemical composition of *Enterococcus faecalis* in biofilm cells initiated from different physiologic states," *Folia Microbiologica*, vol. 59, no. 5, pp. 447–453, 2014.
- [21] J. F. Siqueira, I. N. Rôças, and D. Ricucci, "Biofilms in endodontic infection," *Endodontic Topics*, vol. 22, no. 1, pp. 33–49, 2012.

- [22] J. M. Guerreiro-Tanomaru, N. B. de Faria-Júnior, M. A. H. Duarte, R. Ordinola-Zapata, M. S. Z. Graeff, and M. Tanomaru-Filho, "Comparative analysis of *Enterococcus faecalis* biofilm formation on different substrates," *Journal of Endodontics*, vol. 39, no. 3, pp. 346–350, 2013.
- [23] A. Kishen, M. Upadya, G. P. Tegos, and M. R. Hamblin, "Efflux pump inhibitor potentiates antimicrobial photodynamic inactivation of *Enterococcus faecalis* biofilm," *Photochemistry and Photobiology*, vol. 86, no. 6, pp. 1343–1349, 2010.
- [24] M. Martins, P. Uppuluri, D. P. Thomas et al., "Presence of extracellular DNA in the *Candida albicans* biofilm matrix and its contribution to biofilms," *Mycopathologia*, vol. 169, no. 5, pp. 323–331, 2009.
- [25] L. A. Reisner, A. Cao, and A. K. Pandya, "An integrated software system for processing, analyzing, and classifying Raman spectra," *Chemometrics and Intelligent Laboratory Systems*, vol. 105, no. 1, pp. 83–90, 2011.
- [26] J. A. Mohamed, W. Huang, S. R. Nallapareddy, F. Teng, and B. E. Murray, "Influence of origin of isolates, especially endocarditis isolates, and various genes on biofilm formation by *Enterococcus faecalis*," *Infection and Immunity*, vol. 72, no. 6, pp. 3658–3663, 2004.
- [27] J. A. T. Sandoe, J. Wymore, A. P. West, J. Heritage, and M. H. Wilcox, "Measurement of ampicillin, vancomycin, linezolid and gentamicin activity against enterococcal biofilms," *Journal of Antimicrobial Chemotherapy*, vol. 57, no. 4, pp. 767–770, 2006.
- [28] Z. T. Wen, D. Yates, S.-J. Ahn, and R. A. Burne, "Biofilm formation and virulence expression by *Streptococcus mutans* are altered when grown in dual-species model," *BMC Microbiology*, vol. 10, no. 1, p. 111, 2010.
- [29] J. Makovcova, V. Babak, P. Kulich, J. Masek, M. Slany, and L. Cincarova, "Dynamics of mono- and dual-species biofilm formation and interactions between *Staphylococcus aureus* and gram-negative bacteria," *Microbial Biotechnology*, vol. 10, no. 4, pp. 819–832, 2017.
- [30] M. I. Klein, J. Xiao, B. Lu, C. M. Delahunty, J. R. Yates, and H. Koo, "*Streptococcus mutans* protein synthesis during mixed-species biofilm development by high-throughput quantitative proteomics," *PLoS One*, vol. 7, no. 9, Article ID e45795, 2012.
- [31] F. Dubois-Brissonnet, E. Trotier, and R. Briandet, "The biofilm lifestyle involves an increase in bacterial membrane saturated fatty acids," *Frontiers in Microbiology*, vol. 7, p. 1673, 2016.
- [32] Y. Chao and T. Zhang, "Surface-enhanced Raman scattering (SERS) revealing chemical variation during biofilm formation: from initial attachment to mature biofilm," *Analytical and Bioanalytical Chemistry*, vol. 404, no. 5, pp. 1465–1475, 2012.
- [33] W. E. Huang, R. I. Griffiths, I. P. Thompson, M. J. Bailey, and A. S. Whiteley, "Raman microscopic analysis of single microbial cells," *Analytical Chemistry*, vol. 76, no. 15, pp. 4452–4458, 2004.
- [34] A. M. T. Barnes, K. S. Ballering, R. S. Leibman, C. L. Wells, and G. M. Dunny, "Correlative ultrastructural analysis of extracellular DNA in early *Enterococcus faecalis* biofilms," *Microscopy and Microanalysis*, vol. 18, no. 2, pp. 8–9, 2012.
- [35] A. M. Gonzalez, E. Corpus, A. Pozos-Guillen, D. Silva-Herzog, A. Aragon-Piña, and N. Cohenca, "Continuous drip flow system to develop biofilm of *E. faecalis* under anaerobic conditions," *Scientific World Journal*, vol. 2014, Article ID 706189, 5 pages, 2014.
- [36] M. Sena-Vélez, C. Redondo, J. H. Graham, and J. Cubero, "Presence of extracellular DNA during biofilm formation by *Xanthomonas citri* subsp. *citri* strains with different host range," *PLoS One*, vol. 11, no. 6, Article ID e0156695, 2016.
- [37] M. Okshesky and R. L. Meyer, "The role of extracellular DNA in the establishment, maintenance and perpetuation of bacterial biofilms," *Critical Reviews in Microbiology*, vol. 41, no. 3, pp. 341–352, 2013.
- [38] T. Ramirez-Mora, C. Retana-Lobo, and G. Valle-Bourrouet, "Biochemical characterization of extracellular polymeric substances from endodontic biofilms," *PLoS One*, vol. 13, no. 11, Article ID e0204081, 2018.
- [39] L. E. Chávez de Paz, J. R. Davies, G. Bergenholtz, and G. Svensäter, "Strains of *Enterococcus faecalis* differ in their ability to coexist in biofilms with other root canal bacteria," *International Endodontic Journal*, vol. 48, no. 10, pp. 916–925, 2015.
- [40] C. You-Peng, Z. Peng, G. Jin-Song, F. Fang, X. Gao, and C. Li, "Functional groups characteristics of EPS in biofilm growing on different carriers," *Chemosphere*, vol. 92, no. 6, pp. 633–638, 2013.
- [41] J. De Gelder, K. De Gussem, P. Vandenabeele, P. De Vos, and L. Moens, "Methods for extracting biochemical information from bacterial Raman spectra: an explorative study on *Cupriavidus metallidurans*," *Analytica Chimica Acta*, vol. 585, no. 2, pp. 234–240, 2007.
- [42] C. A. Guzmán, C. Pruzzo, G. LiPira, and L. Calegari, "Role of adherence in pathogenesis of *Enterococcus faecalis* urinary tract infection and endocarditis," *Infection and Immunity*, vol. 57, no. 6, pp. 1834–1838, 1989.
- [43] K. L. Palmer, P. Godfrey, A. Griggs et al., "Comparative genomics of enterococci: variation in *Enterococcus faecalis*, clade structure in *E. faecium*, and defining characteristics of *E. gallinarum* and *E. casseliflavus*," *mBio*, vol. 3, no. 1, article e00318-11, 2012.
- [44] B. Rosan and B. F. Hammond, "Extracellular polysaccharides of *Actinomyces viscosus*," *Infection and Immunity*, vol. 10, no. 2, pp. 304–308, 1974.
- [45] J. N. C. Fong and F. H. Yildiz, "Biofilm matrix proteins," *Microbiology Spectrum*, vol. 3, no. 2, pp. 1–23, 2015.
- [46] A. Taglialegna, I. Lasa, and J. Valle, "Amyloid structures as biofilm matrix scaffolds," *Journal of Bacteriology*, vol. 198, no. 19, pp. 2579–2588, 2016.
- [47] J. López-Ochoa, J. F. Montes-García, C. Vázquez et al., "*Gallibacterium* elongation factor-Tu possesses amyloid-like protein characteristics, participates in cell adhesion, and is present in biofilms," *Journal of Microbiology*, vol. 55, no. 9, pp. 745–752, 2017.
- [48] A. Rygula, K. Majzner, K. M. Marzec, A. Kaczor, M. Pilarczyk, and M. Baranska, "Raman spectroscopy of proteins: a review," *Journal of Raman Spectroscopy*, vol. 44, no. 8, pp. 1061–1076, 2013.
- [49] D. Kurouski, R. P. Van Duyn, and I. K. Lednev, "Exploring the structure and formation mechanism of amyloid fibrils by Raman spectroscopy: a review," *Analyst*, vol. 140, no. 15, pp. 4967–4980, 2015.
- [50] K. Czamara, K. Majzner, M. Z. Pacia, K. Kochan, A. Kaczor, and M. Baranska, "Raman spectroscopy of lipids: a review," *Journal of Raman Spectroscopy*, vol. 46, no. 1, pp. 4–20, 2014.
- [51] M. Reich, K. Kümmerer, A. Al-Ahmad, and C. Hannig, "Fatty acid profile of the initial oral biofilm (pellicle): an in-situ study," *Lipids*, vol. 48, no. 9, pp. 929–937, 2013.



Hindawi

Submit your manuscripts at
www.hindawi.com

